Developmental Cell, Vol. 3, 1–20, November, 2002, Copyright ©2002 by Cell Press

Sequential Activation of Signaling Pathways during Innate Immune Responses in *Drosophila*

Michael Boutros,[1,4] Hervé Agaisse,[1,2,4] and Norbert Perrimon[1,2]
[1]Department of Genetics
[2]Howard Hughes Medical Institute
Harvard Medical School
200 Longwood Avenue
Boston, Massachusetts 02115

Summary

Innate immunity is essential for metazoans to fight microbial infections. Genome-wide expression profiling was used to analyze the outcome of impairing specific signaling pathways after microbial challenge. We found that these transcriptional patterns can be dissected into distinct groups. We demonstrate that, in addition to signaling through the Toll and Imd pathways, signaling through the JNK and JAK/STAT pathways controls distinct subsets of targets induced by microbial agents. Each pathway shows a specific temporal pattern of activation and targets different functional groups, suggesting that innate immune responses are modular and recruit distinct physiological programs. In particular, our results may imply a close link between the control of tissue repair and antimicrobial processes.

Introduction

Innate immunity is an ancient biological process that multicellular organisms use for their defense against pathogenic challenges. First-line defense mechanisms are found in various evolutionarily distant metazoans, from plants to humans (reviewed in Hoffmann et al., 1999). In higher vertebrates, innate immunity is an integral part of the host defense system that triggers the expression of costimulatory molecules, whereas invertebrates rely exclusively on innate mechanisms for protection against infectious agents (Schnare et al., 2001; reviewed in Akira et al., 2001; Fearon and Locksley, 1996; Janeway, 1989).

In recent years, Toll-like receptors (TLRs) have been shown to play a crucial role in innate immunity (reviewed in Aderem and Ulevitch, 2000; Kimbrell and Beutler, 2001). Toll was initially identified in *Drosophila* to be required for the establishment of embryonic dorsoventral polarity (Anderson et al., 1985). Later studies demonstrated that Toll mediates fungal and gram-positive-specific immune responses (Lemaitre et al., 1996). In mammals, TLRs recognize pathogen-specific markers, such as lipopolysaccharides (TLR4), peptidoglycans (TLR2), and viral double-stranded RNA (TLR3; Alexopoulou et al., 2001; Hayashi et al., 2001; Poltorak et al., 1998; Takeuchi et al., 1999). In *Drosophila*, two distinct NFκB signaling pathways are activated upon microbial infection. In response to gram-positive and fungal infection, Toll triggers a transcriptional response through the death domain-containing protein Tube (Tub), the IRAK-like protein kinase Pelle (Pll), and the IκB-like inhibitor factor Cactus (Cact; Lemaitre et al., 1995b, 1996). The inactivation of Cact leads to the translocation of the NFκB transcription factor Dif and induction of antimicrobial target genes. Gram-negative bacteria signal through a distinct pathway, referred to as the Imd pathway (Lemaitre et al., 1995a). Downstream of a receptor, the signal is relayed by Imd, IKKβ, and IKKγ (encoded by *key*) and Relish (Rel) (Georgel et al., 2001; Hedengren et al., 1999; Lu et al., 2001; Silverman et al., 2000; Vidal et al., 2001).

One of the fundamental questions in signal transduction is, how are extracellular signals transmitted through a network of components to control specific cellular functions? Many signaling pathways, such as Toll pathways, are reutilized for different cellular programs. However, the mechanisms by which pathways establish their specificity remains largely unresolved. Microarray analysis has been widely used to investigate changes in gene expression levels that may be indicative of specific biological programs. In yeast, expression analysis has revealed that genes operating in a common process, such as mitosis or replication, are often tightly coregulated (Chu et al., 1998). Recently, several studies have investigated the transcriptional response to microbial infections in *Drosophila* (De Gregorio et al., 2001; Irving et al., 2001). While it is well established that NFκB-dependent signaling pathways play a central role in innate immune responses, the role of other signaling events remains poorly understood.

Here, we use expression profiling and loss-of-function experiments to analyze signaling pathways that control microbial challenge-induced transcriptional patterns. We find that dynamic patterns after LPS stimulation and septic injury can be dissected into distinct, signaling pathway-specific responses. These signaling signatures appear with discrete temporal patterns, revealing a link between pathway activation and temporal organization that can be used to predict the activation of distinct signaling pathways. Our data indicates that, in addition to the Toll and Imd pathways, the JNK and JAK/STAT pathways contribute to the expression of microbial challenge-induced genes. Each pathway's target set is enriched for genes of specific functional groups, indicating that these signaling pathways fulfill separate functions after microbial infection. Our results reveal a connection of pathway targets and temporal patterns and indicate a close link between antimicrobial peptide expression and the induction of cytoskeletal remodeling.

Results

Signaling in Response to Lipopolysaccharides

Lipopolysaccharides (LPS) are the principal cell wall components of gram-negative bacteria. In mammals,

[3]Correspondence: perrimon@rascal.med.harvard.edu
[4]These authors contributed equally to this work.

exposure to LPS causes septic shock through a TLR4-dependent signaling pathway (Poltorak et al., 1998). LPS treatment of *Drosophila* SL2 cells leads to rapid expression of antimicrobial peptides, such as Cecropins (Cec; Samakovlis et al., 1992). SL2 cells resemble embryonic hemocytes and have also been used as a model system to study JNK and other signaling pathways (Han and Ip, 1999; Sluss et al., 1996). LPS-responsive induction of the antimicrobial peptides AttacinA (AttA), Diptericin (Dipt), and Cec was shown to rely on IKK and Relish (Silverman et al., 2000). In order to obtain a broad overview on the transcriptional response to LPS in *Drosophila*, we generated genome-wide expression profiles of SL2 cells at different time points following LPS treatment.

Figure 1A shows the hierarchical clustering of 238 genes that passed our filtering criteria (see Experimental Procedures). In time-course experiments, we observed a complex pattern of gene expression that can be separated into different temporal clusters. A first group, with peak expression at 60 min after LPS, primarily consists of cytoskeletal regulators, signaling, and proapoptotic factors. This group includes cytoskeletal and cell adhesion modulators such as Matrix metalloprotease-1, WASp, Myosin, and Ninjurin, proapoptotic factors such as Reaper, and signaling proteins such as Puckered and VEGF-2. A second group, with peak expression at 120 min, includes many known defense and immunity genes, such as Cec, Mtk, and AttA, but not the gram-positive-induced peptide Drs. Interestingly, this cluster also includes PGRP-SA, which is a gram-positive pattern recognition receptor in vivo (Michel et al., 2001), suggesting possible crossregulation between gram-positive- and gram-negative-induced factors. A third group is transiently downregulated upon LPS stimulation. This cluster includes genes that play a role in cell cycle control, such as String and Rca1 (see also Figure 1B and Supplemental Data at http://www.developmentalcell.com/cgi/content/full/3/5/■■■/DC1). Altogether, our results show that, in response to LPS, a defined gram-negative stimulus, cells elicit a complex transcriptional response.

JNK and Rel Signals Branch Downstream of Tak1

In adult *Drosophila*, gram-negative bacteria elicit an antimicrobial response mediated by a signaling pathway that involves the intracellular factors Imd, Tak1, Key, and Rel (Georgel et al., 2001; Hedengren et al., 1999; Lu et al., 2001; Vidal et al., 2001). On the basis of our previous results, we reasoned that the temporal waves of transcriptional activity in SL2 cells might reflect different signaling pathway contributions. We therefore asked whether selectively removing signaling components by RNA interference (RNAi) would block induction of all, or only parts, of the transcriptional response to LPS.

We first investigated the effect of removing *key* or *rel* by RNAi. As shown in Figure 2A, the expression profiles demonstrated that removing *key* or *rel* diminished the induction of antimicrobial peptides. However, the induction of cytoskeletal and proapoptotic factors was not affected. In contrast, removing *tak1* reduced the level of induction or repression for all identified genes (Figure 2A), indicating that LPS-induced signaling is transmitted through Tak1 and that specific pathways branch downstream of Tak1.

In the Rel-independent group, we identified several transcripts that were indicative of other signaling events. For example, *puc* is transcriptionally regulated by JNK signaling during embryonic development (Martin-Blanco et al., 1998). Therefore, we tested the effect of removing SAPK/JNK activity on LPS-induced transcripts. As shown in Figure 2A, *mkk4/hep* dsRNA-treated cells loose the ability to induce the Rel-independent cluster, indicating that LPS signaling branches downstream of Tak1 into separate Rel- and JNK-dependent branches (see also Figure 2B). To validate the results obtained from the microarray experiments, we performed quantitative PCR (qPCR) using *puc* and *cec* mRNA levels as indicators for Imd/Rel- or Mkk4/Hep-dependent pathways. Additionally, we tested the effect of removing *imd*, which, in vivo, acts upstream of Tak1, to clarify whether, in addition to Tak1, other known upstream components of a gram-negative signaling pathway are required for both Rel- and Mkk4/Hep-dependent pathways (Georgel et al., 2001; Vidal et al., 2001). These qPCR experiments confirmed that *cec* is dependent for its expression on Imd, Tak1, Rel, and Key, whereas LPS-induced *puc* expression is dependent on Imd, Tak1, and Mkk4/Hep (Figure 2C). Hence, the immunity signaling pathway in response to LPS bifurcate downstream of Imd and Tak1 into Rel- and SAPK/JNK-dependent branches. Both the Rel and SAPK/JNK pathways regulate different functional groups of downstream target genes.

While both Rel and Mkk4/Hep pathways are downstream of Imd and Tak1 in response to LPS, the two downstream branches elicit different temporal expression patterns. We then asked whether the first transcriptional response is controlled by downstream targets that might negatively feed back into the signaling circuit. *puc* was a candidate for such a transcriptionally induced negative regulator. We therefore compared expression profiles of cells depleted for *puc* before and after a 60 min LPS treatment. As shown in Figure 3A, these experiments showed that transcripts dependent on the Mkk4/Hep branch of LPS signaling were upregulated, even without further LPS stimulus. In contrast, Rel branch targets were not influenced (Figure 3A). We also noticed that *puc* dsRNA-treated cells show loss of the typical round cell shape. These cells appear flat and have a delocalized Actin staining (Figure 3B), consistent with a deregulation of cytoskeletal modulators in *puc*-deficient cells.

The analysis of expression profiles showed that, while SAPK/JNK and Rel signaling are controlled by the same Imd/Tak1 cascade, they appear to have different feedback loops. Whereas Rel signaling induces Rel expression and thereby generates a self-sustaining loop, possibly leading to the maintenance of target gene expression, the SAPK/JNK branch induces an inhibitor and thereby establishes a self-correcting feedback loop. These results may explain how a single upstream cascade can lead to different dynamic patterns.

Septic Injury Induces Multiple Distinct Temporal Sets of Target Genes

Septic injury of adult *Drosophila* is a widely used model system to study innate immune responses in vivo (Lemaitre et al., 1995a, 1996). To explore the signaling

A

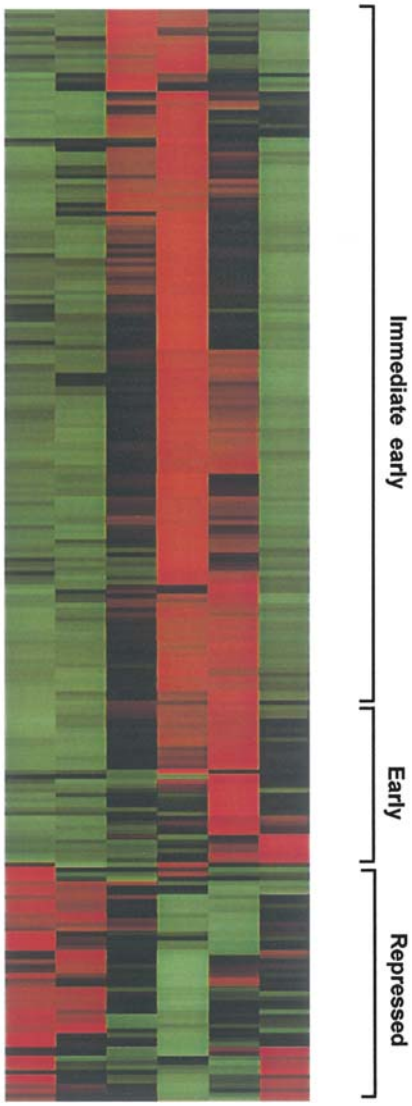

B

EARLY GROUP probeset	Name	Δ MBE	MBE Ratio 30min	60min	120min
143096_f_at	Cecropin A1	14493	29.2	41.1	46.2
143097_f_at	Cecropin A2	10412	54.0	76.4	95.1
147220_s_at	Attacin B1	9859	13.2	27.3	42.7
143609_at	Drosocin	5152	9.4	25.1	59.2
143770_at	Metchnikowin	4539	20.3	58.9	167.8
150090_at	Attacin D	4243	6.5	33.4	66.1
141374_at	Attacin-A	3967	9.0	19.3	43.6
147473_at	Diptericin B	3695	2.3	5.4	20.6
144882_at	PGRP-SA	2539	1.9	2.6	3.5
153921_at	Kenny (IKK)	465	1.3	1.4	1.7
143100_f_at	Cecropin C	99	2.2	3.3	4.5

IMMEDIATE EARLY GROUP probeset	Name	Δ MBE	MBE Ratio 30min	60min	120min
147882_at	CG4859 (matrix metalloproteinase)	6498	4.1	12.6	8.2
151822_at	Relish	4057	8.7	11.6	7.1
153673_at	Annexin IX	2957	1.7	2.3	2.3
146650_at	CG11066 (serine-type endopeptidase)	1969	1.9	4.5	3.0
153546_at	Fimbrin (actin binding protein)	1928	1.3	2.1	1.9
145941_at	VEGF-related factor 2	1374	1.1	5.2	2.8
155144_at	CG1049 (cholinephosphate cytidylyltransferase)	1272	1.4	2.0	1.6
146880_at	wunen-2	1188	1.7	4.7	3.1
141620_at	RhoL	1169	1.5	1.9	0.9
141732_at	puckered	1118	3.1	3.7	1.4
154320_at	Jun	1100	2.3	2.9	1.6
146286_at	CG5446 (heat shock factor binding protein)	1061	1.6	1.9	2.3
146651_at	CG15900 (serine-type endopeptidase)	1010	2.0	3.5	2.6
152300_at	CG18593 (Thioredoxin-like)	1009	1.5	2.1	2.2
142975_at	Myosin 31DF	962	1.3	1.8	1.5
154514_at	Cortactin	881	1.4	1.8	1.6
148533_at	CG6449 (Ninjurin-like)	733	2.6	3.0	2.3
147954_at	Trio (RhoGEF)	664	1.8	2.5	1.4
153313_at	Rac2	561	1.5	2.1	1.4
154192_at	Dap160 (dynamin associated protein)	532	1.4	1.8	1.3
145970_at	CG18589 (Alpha-2-macroglobulin family)	449	1.9	2.1	1.9
143570_at	Ets21C	433	2.8	4.4	1.8
151599_at	RhoGEF3	290	2.0	2.5	2.8
150785_at	WASp (CG1520)	261	1.2	2.1	1.2
153776_at	Caspase (CG7863)	140	2.1	1.8	1.6
143125_at	Dorsal	119	2.3	1.9	1.0
143680_at	reaper	108	3.3	1.9	2.1
154230_at	CG5797 (Peroxiredoxin)	57	1.0	5.1	3.0

REPRESSED GROUP probeset	Name	Δ MBE	MBE Ratio 30min	60min	120min
141264_at	string	1086	0.4	0.3	0.7
154293_at	Dom	216	0.7	0.5	0.7
152549_at	Rca1 (Regulator of cyclin A1)	199	0.7	0.6	1.0
143248_at	HLHm3	195	0.4	0.4	0.5
143438_at	Serrate	167	0.7	0.4	0.6

Figure 1. Lipopolysaccharides Induced Expression Patterns in SL2 Cells

(A) Hierarchical clustering diagram of 238 filtered genes. Expression profiles were generated after LPS treatment for the indicated times. Data analysis was performed with a model-based algorithm implemented in dChip. Expression values in gene rows are mean centered, normalized to have a variation of 1, and hierarchically clustered (Eisen et al. 1998). Different shades of green represent model-based expression values between 0 and 3 standard deviations below the mean value, and shades of red represent expression values between 0 and 3 standard deviations above the mean value. Note that "immediate early" and "early" clusters are clearly distinguished by the timing of their peak expression levels.

(B) Table of differentially regulated genes. ΔMBE indicates the difference between the highest and lowest expression values. The column "MBE Ratio" shows the ratio of expression at the indicated time point compared with nonstimulated cells. Note that genes in the early cluster show peak expression at 120 min after LPS treatment, whereas genes in the immediate early cluster show peak expression at 60 min or earlier. See Supplemental Data at http://www.developmentalcell.com/cgi/content/full/3/5/■■■/DC1 for a complete listing.

pathways that control induced genes in vivo, we first generated genome-wide expression profiles of adult *Drosophila* infected by septic injury. Equal numbers of male and female adult Oregon R flies were infected with a mixture of *E. coli* (gram negative) and *M. luteus* (gram positive). Subsequently, flies were collected at 1, 3, 6, 24, 48, and 72 hr time points post-septic injury to measure temporal changes in gene expression levels. Computational analysis identified a list of 223 genes that were differentially regulated and matched our filtering criteria for at least two time points after microbial infection (see Experimental Procedures). This set includes 197 genes that are transiently upregulated and 26 that are transiently downregulated upon immune challenge (see

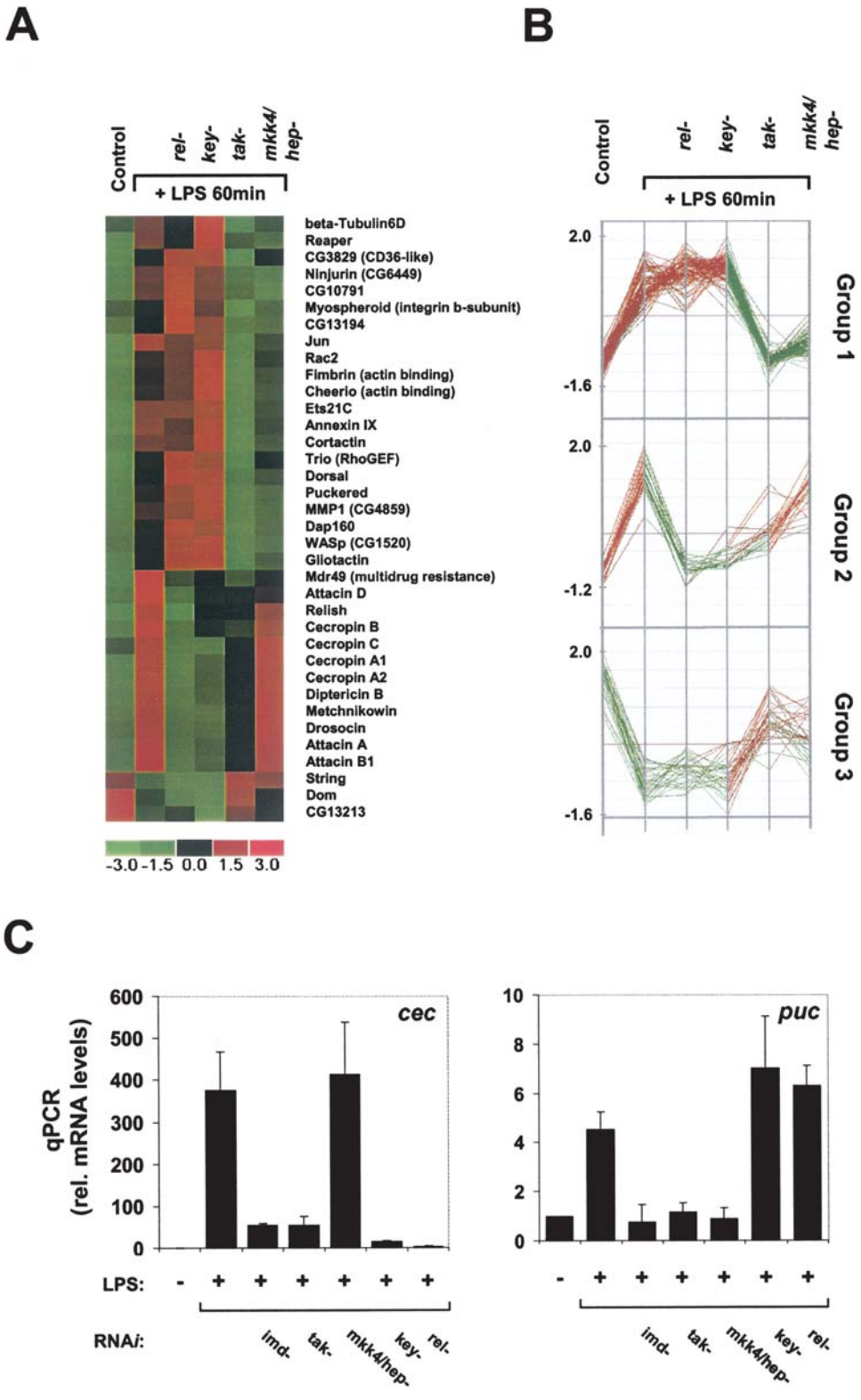

Figure 2. Differential Requirement of Cytoskeletal and Antimicrobial Genes for SAPK/JNK and Rel Pathways

(A) Representation of relative expression levels of Key/Rel- and Mkk4/Hep-dependent transcripts. Cells were treated with the indicated dsRNA for 72 hr prior to a 60 min LPS stimulation. Extracted total RNA was labeled and hybridized to oligonucleotide arrays. Depletion of *tak1* reduces the expression of all LPS-inducible transcripts, whereas depletion of *rel* or *mkk4/hep* abolishes the expression of separate sets of induced transcripts. Color scales are as described in Figure 1.

(B) Overall expression patterns of three differentially regulated groups of genes. Cells were treated for 72 hr with dsRNA against *tak1*, *key*, *rel*, and *mkk4/hep*. Cells were then stimulated for 60 min with LPS. Ratios of expression values were normalized over their variance. Genes

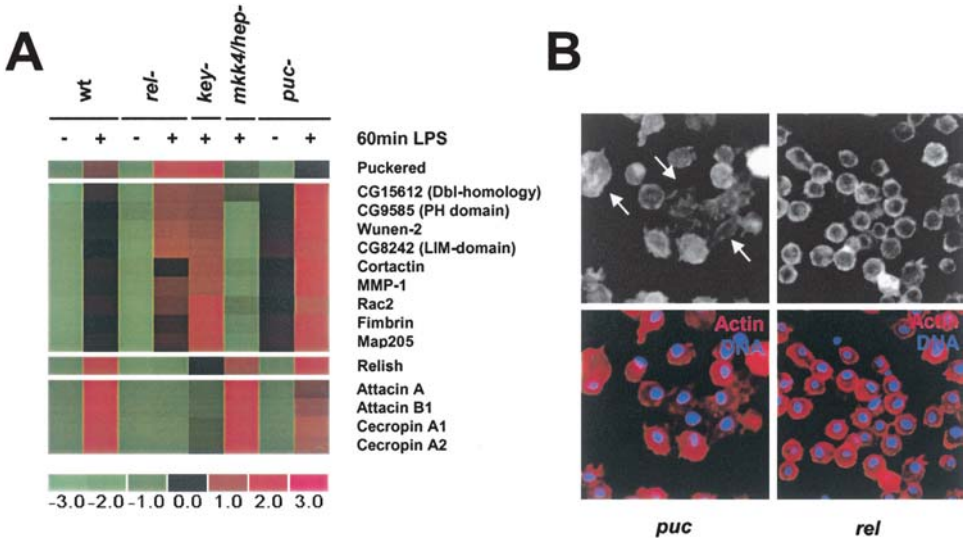

Figure 3. Puckered Negatively Controls the SAPK/JNK Branch of LPS Signaling and Derepresses Cytoskeletal Genes

(A) Representation of model-based expression levels. Colors are as described in Figure 1. Removal of *puc* in SL2 cells leads to the constitutive expression of SAPK/JNK pathway-dependent genes, even without LPS stimulus. In contrast, removing *rel* without LPS stimulation does not lead to constitutive expression of cytoskeletal genes.

(B) *puc* removal induces cell shape changes. SL2 cells were treated with dsRNA against *puc* or *rel*. Cells were subsequently washed in PBS, fixed in 4% formaldehyde for 20 min at room temperature, and permeabilized with PBST. Actin was visualized with Alexa 568 phalloidin (Molecular Probes), and DNA was visualized by DAPI (Sigma) staining.

Supplemental Figure S3). Different temporal profiles of gene expression can be detected in our analysis; clusters of genes differed significantly in the timing and persistence of induction. For example, whereas many genes are expressed transiently shortly after infection (see Supplemental Figure S3), others are induced late and are still upregulated at a 72 hr time point. A significant number of genes of both early and late clusters were differentially expressed at a 6 hr time point after infection, which we chose for further analysis.

We then examined the signaling requirements for these differentially expressed transcripts in mutant alleles of known Toll and Imd/Rel pathway components, reasoning that we might uncover additional pathways by analyzing patterns that cannot be reconciled with expected signaling patterns. Flies homozygous for loss-of-function mutations in *tub*, *key*, or *rel* were infected with gram-negative and gram-positive bacteria, and expression profiles were generated for a 6 hr time point after infection. In addition, noninfected *Tl*^{10b}, a gain-of-function allele of the receptor, and *cact,* a homolog of the inhibitory factor IκB, were used to monitor transcripts that are constitutively expressed in gain-of-function signaling mutants. The antimicrobial peptides *dipt* and *drosomycin* (*drs*) are representative targets for the Toll and Imd/Rel pathways, respectively (Lemaitre et al., 1995a, 1996). As previously shown, *dipt* induction is not detectable in our expression profiles in either a *rel* or *key* mutant background, whereas its expression is not affected in *tub* mutants (Figure 4B). In contrast, *drs* relies on Tub to convey a Toll-dependent signal. Consistently, our expression profiles show that, in a *tub* mutant background, *drs* expression is diminished (Figure 4B). These experiments showed that the analysis of our mutant expression profiles can be used to deduce signaling requirements for distinct target groups.

Toward a computational annotation of signaling pathways, we employed a pattern-matching strategy to rank transcripts by similarity to bona fide Toll or Imd/Rel pathway targets, such as *dipt* and *drs*. We analyzed a set of 91 transcripts that matched our filtering criteria for differential expression at a 6 hr time point after septic injury. To determine their dependence on known immunity signaling pathways, we calculated the correlation coefficients of the individual gene expression level in mutant backgrounds to binary Toll or Imd/Rel patterns (Table 1). Genes were subsequently ordered according to their correlation coefficients for each pathway signature. Using this strategy, we separated transcripts that primarily belong to either the Toll or Imd/Rel pathway groups (Figures 4C and 4D). For example, genes that show a high correlation coefficient for a Toll pathway

in group 1 are independent of Rel and Key but are dependent on Tak and MKK4/Hep for their induction after LPS treatment. Group 2 genes are expressed independently of MKK4/Hep but are dependent on Tak, Rel, and Key for their expression. Group 3 genes are repressed after LPS treatment. The repression is not affected by Rel and Key, but they are not repressed by Tak and are partially repressed by MKK4/Hep.

(C) Quantitative PCR analysis for *cec* (left panel) and *puc* (right panel) as indicators for Rel and SAPK/JNK signaling pathways. Cells were treated with dsRNA for *imd*, *tak1*, *key*, *rel*, and *mkk4/hep* and harvested for total RNA extraction. Left panels show fold changes (FC) calculated from quantitative PCR results with *rp49* as internal normalization control. Treatment with both *mkk4* and *hep* dsRNA was necessary to reduce *puc* expression. Depletion of either *mkk4* or *hep* alone led to a partial reduction of induced *puc* levels (data not shown).

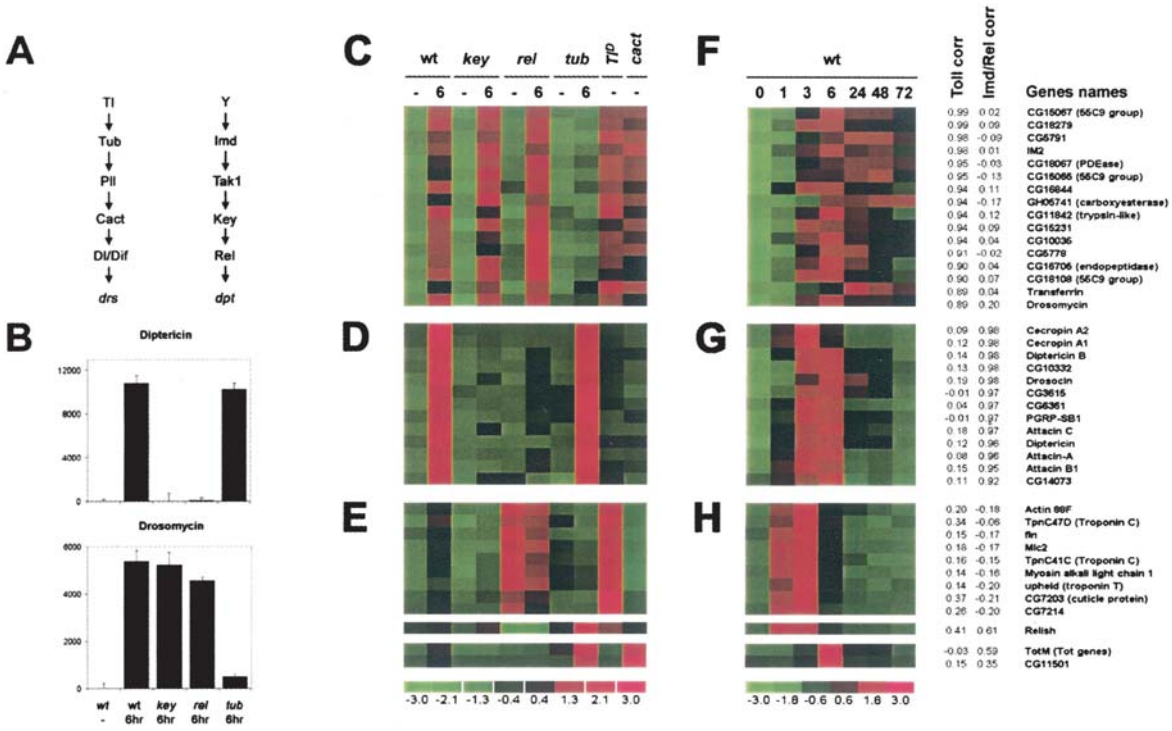

Figure 4. Signaling Pathway Requirements Correlate with Distinct Temporal Expression Profiles

(A) Schematic of Toll and Imd/Rel pathways activated during innate immunity in *Drosophila*.

(B) Expression values of *dipt* and *drs* in different genetic backgrounds. Differences between expression levels in infected and noninjured *Drosophila* wild-type or mutants were plotted. wt, Oregon R; *key*, key^{1}/key^{1}; *rel*, rel^{E20}/rel^{E20}; *tub*, tub^{118}/tub^{238}; *cact*, $cact^{EH9}/cact^{A2}$; Tl^{D}, $Tl^{10b}/+$.

(C–E) A representation of model-based expression levels. The left panels show the expression levels of genes in different mutant backgrounds. The right panels show the expression levels during the time course of infection. Expression values in gene rows in each panel were mean centered and variance normalized. Different shades of green represent an expression value between 0 and 3 standard deviations below the mean expression value, and shades of red represent an expression value between 0 and 3 standard deviations above the mean expression value. The column "Toll-corr" shows the correlation coefficient of the indicated genes with the binary Toll signaling pattern in Table 1. The column "Imd/Rel-corr" shows the correlation coefficient of the indicated genes with a bona fide Imd/Rel target gene. A value of 1 indicates a perfect match. A cutoff of 0.75 was used for selecting genes in (C) and (D) (see Supplemental Figure S4 at http://www.developmentalcell.com/cgi/content/full/3/5/■■■/DC1 for full diagrams). Both panels show the highest-scoring genes ranked according to their correlation coefficients.

(C) Genes that score high for similarity with the Toll pathway, but low for the Imd/Rel pathway signature. These transcripts are dependent on *tub* for their induction after microbial challenge and are constitutively expressed in Tl^{10b} and *cac*, but they are not affected in *key* and *rel* mutants.

(D) Genes rank high for Imd/Rel, but low for Toll signature similarity. These transcripts are dependent on *key* and *rel* for their induction after microbial challenge, are independent of *tub*, and are not constitutively expressed in Tl^{10b} and *cac*.

(E) Transcripts that score low for both Toll and Imd/Rel pathway signatures.

(F–H) Corresponding temporal patterns.

pattern include *drs*, *transferrin*, a secreted iron binding protein, IM2, and a cluster of homologous secreted peptides at 55C9 (Figure 4C). These genes have a low correlation coefficient for an Imd/Rel pattern, indicating that they are primarily dependent on Toll pathway signaling in response to microbial infection. In contrast, the genes shown in Figure 4D score low for a Toll pathway pattern but have high correlation coefficients for an Imd/Rel pattern. This group includes known gram-negative antimicrobial peptides, such as *cec* and *dipt*, *peptidoglycan receptor-like* genes (*PGRP-SD, PGRP-SB1*), other small transcripts (*CG10332*), and genes coding for putative transmembrane proteins, such as *CG3615* (see Supplemental Data for complete listing).

Interestingly, some genes do not fit either pattern, suggesting that they are regulated by other pathways. One group of genes, including cytoskeletal factors such as *actin88F*, *flightin*, and *tpnC41C*, is induced in Tl^{10b}, but not in *cact*, mutants. In contrast, *totM* (Ekengren and Hultmark, 2001) and *CG11501* are expressed at high levels in *cact* mutant flies but are not expressed in Tl^{10b} mutant flies. In addition, these transcripts are highly inducible in a *tub* genetic background, but they are not inducible in *key* or *rel*. This may suggest that Toll, Tub, and Cact do not act in a linear pathway under all circumstances. Moreover, *rel* shows an expression pattern suggesting that it is regulated by both the Imd/Rel and Toll pathways (Figure 4E). Thus, these results indicate that, in addition to the canonical Toll and Imd pathways, other signaling events and possibly signaling pathway branching contribute to the complex expression patterns after septic injury (see derived patterns in Table 1). Finally, we note that there is a strong correlation between pathway requirement and temporal expression pattern. Whereas Toll targets are exclusively found in the sustained cluster, Imd/Rel targets are expressed

Table 1. Binary Patterns for Assigning Targets to Known and Derived Signaling Pathway Signatures

Pathway Patterns	wt	wt (6 hr)	*key*	*key* (6 hr)	*rel*	*rel* (6 hr)	*tub*	*tub* (6 hr)	*Tl10b*	*cact*	Number of Genes	Examples
Search patterns												
Toll group	0	1	0	1	0	1	0	0	1	1	28	*drs*, *im2*, *CG16836*
imd/*rel* group	0	1	0	0	0	0	0	1	0	0	22	*cec*, *dpt*, *attA*, *CG3615*
Derived patterns												
cyto group	0	1	0	0	1	1	0	0	1	0	12	*act88F*, *fln*, *mlc*, *CG7214*
totM group	0	1	0	0	0	0	0	1	0	1	2	*totM*, *CG11501*
Others												
Repressed											4	*Sodh-1*, *CG18030*
Other											23	*relish*, *CG18589*

For each pathway signature, binary expression levels in different mutant backgrounds are listed. Search patterns were used to calculate correlation coefficients and rank transcripts in descending order. We set a cutoff of 0.75 for genes to be counted in the "Number of Genes" column. New patterns from transcripts that could not be assigned to either Toll or Imd/Rel target patterns. Genes that did not match the criteria and have not been assigned are listed in "Others." For a complete listing and expression levels, see Supplemental Data at http://www.developmentalcell.com/cgi/content/full/3/5/■■■/DC1.

early and transiently after septic injury. The two additional clusters with noncanonical patterns show temporal patterns distinct from either Toll or Imd pathways (Figures 4F–4H).

JNK and JAK/STAT Signaling Control Subsets of Septic Injury-Induced Genes

We reasoned that the patterns observed in our mutant analysis might reflect the contributions of additional signaling pathways. Also, these noncanonical clusters show distinct temporal expression patterns (Figure 4E and Table 1), suggesting that they are separately controlled. One group of genes consists primarily of cytoskeletal regulators and structural proteins that are expressed early on, with peak expression at 3 hr. These include several muscle-specific proteins, thus possibly reflecting the organ that is injured during injection. For example, *fln* encodes a cytoskeletal structural protein expressed in the indirect flight muscle (Reedy et al., 2000).

Since our previous results demonstrated that the expression of cytoskeletal genes after LPS stimulation is dependent on a JNK cascade, we examined whether removing JNK activity in vivo affects the induction of *fln*. In *Drosophila*, JNK signaling pathways have been previously implicated in epithelial sheet movements during embryonic and pupal development, a process that has been likened to wound-healing responses (Jacinto et al., 2001; Ramet et al., 2002). Our results indicate that in *hep*[1] (JNKK) mutants, which are impaired in JNK

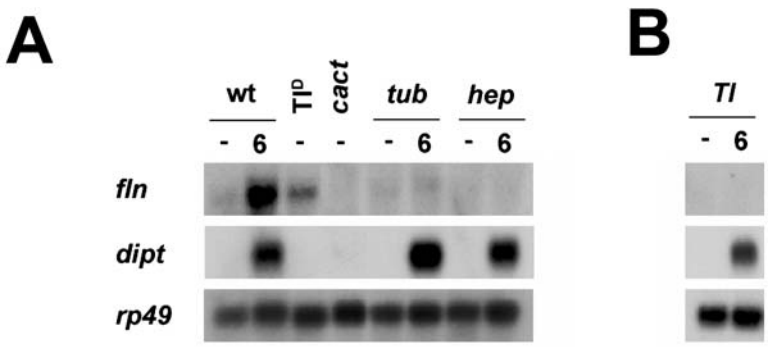

Figure 5. JNK and JAK/STAT Signaling Control Subsets of Genes during Septic Injury Responses

(A–B) Northern Blot analysis of mutants in Toll and JNK pathways (20 μg of total RNA per lane). The same blot was probed with a *fln*-specific probe, stripped, reprobed with a *dipt* probe, and subsequently reprobed with an *rp49* probe as a loading control. Genotypes used were as follows: wt, Oregon R; *tub*, tub^{118}/tub^{238}; *cact*, $cact^{EH9}/cact^{A2}$; Tl^{D}, $Tl^{10b}/+$; *Tl*, Tl^{r444}/Tl^{9QRE}

(C) Quantitative PCR analysis for *CG11501*, *cec*, and *drs* in wt and *hop* (hop^{msv1}/hop^{M38}) genetic backgrounds.

signaling, the induction of *fln* is diminished, whereas the expression of the antimicrobial peptide *dipt* is not affected (Figure 5A). We then tested whether *fln* induction in *Tl* loss-of-function alleles is affected. These experiments showed that *fln* expression is lost in *Tl* mutants, suggesting that Toll acts upstream of a JNK pathway to induce septic injury-induced target genes (Figure 5B).

The clustering revealed a second noncanonical group with small proteins that are expressed late and transiently with peak expression at 6 hr after septic injury. One of the clustered transcripts, CG11501, encodes a small Cys-rich protein that is 115 amino acids long and is strongly induced after septic injury. By RT-PCR, we confirmed that CG11501 is upregulated after septic injury (Figure 5C). In order to characterize how CG11501 is controlled after microbial challenge, we first undertook a candidate pathway approach. In an independent study, we found that *totM* gene induction, which is part of the same cluster, is dependent on a JAK/STAT signaling pathway (Agaisse et al., in preparation). We therefore examined whether CG11501 induction requires JAK/STAT signaling. Mutations in JAK/STAT pathways in *Drosophila* have been implicated in various processes during embryonic and larval development (Perrimon and Mahowald, 1986; Hou and Perrimon, 1997). In *Anopheles*, STAT is activated in response to bacterial infection (Barillas-Mury et al., 1999). Similarly, gain-of-function STAT has been implicated in the transcriptional control of thiolester proteins (Lagueux et al., 2000). We examined here mutant alleles of *hopscotch* (*hop*), the *Drosophila* homolog of JAK. Quantitative PCR shows that CG11501 induction after septic injury is diminished in *hop* loss-of-function mutants, whereas the expression of Toll and Imd targets *drs*, and *cec* is not affected (Figure 5C).

Discussion

In this study, we have investigated the signaling circuits during innate immunity in adult *Drosophila* and cells. Our results show that, in addition to NFκB signaling pathways, other pathways direct the expression of functionally distinct groups of target genes. Specifically, we show that, in addition to known innate immune cascades, JNK and JAK/STAT are required for the transcriptional response during microbial challenge. We find that one transcriptional signature of small secreted peptides can be traced to JAK/STAT signaling. Additionally, JNK signaling controls cytoskeletal genes after an LPS stimulus and after septic injury in vivo. Both in cells and in vivo, JNK pathways are connected to the same upstream signaling cassette that induces NFκB targets. Altogether, these results suggest that innate immune signaling pathways closely link cytoskeletal remodeling, as required for tissue repair, and direct antimicrobial actions. Our data also provide insights into the connection of temporal patterns and the activation of distinct signaling pathways.

NFκB-Independent Signaling during *Drosophila* Innate Immunity

NFκB pathways play a central role for innate and adaptive immune response in mammals. In innate immune responses, TLRs on dendritic cells recognize microbial agents and activate NFκB, leading to the expression of proinflammatory cytokines and other costimulatory factors required to initiate an adaptive immune response. Additionally, other signaling pathways have been implicated at later stages during immune responses in mammals, but their physiological role in innate immunity remains rather poorly understood. For example, several cytokines, such as IL-6 and IL-11, signal through a JAK/STAT pathway to induce the expression of acute phase proteins (reviewed in Ihle, 2001). Similarly, JNK pathways are activated in response to TNF and IL-1, may lead to the expression of immune modulators, and are required for T cell differentiation (Hambleton et al., 1996, Dong et al., 2000). In *Drosophila*, studies have investigated two distinct NFκB-pathways—Toll and Imd/Rel—that have been shown to mediate gram-positive/fungal and gram-negative responses. Both pathways induce specific antimicrobial peptides and thereby focus the response on the invading microbial agent. Genetic analysis has shown that functions of the NFκB-pathways are separable; *Drosophila* that are mutant for only one of these pathways are susceptible to subgroups of pathogens (Lemaitre et al., 1995a). We have asked here whether we can identify the contribution of NFκB-dependent and, possibly, other signaling pathways by examining global expression profiles. The obtained data set demonstrated that NFκB-independent signaling pathways contribute to the transcriptional patterns observed after microbial infection. Both in cells and in vivo, JNK-dependent targets precede the peak expression of antimicrobial peptides that require NFκB. JAK/STAT targets are induced with a distinct temporal pattern that shows late, but only transient, expression characteristics (Figure 6). The stereotyped pathway patterns after microbial challenge suggest that the correct temporal execution of signaling events, similar to signaling during development, may play an important role in the regulation of homeostasis.

JNK Signaling Controls Cytoskeletal Gene Expression

Strikingly, our experiments show that cytoskeletal gene expression during innate immune responses is controlled by JNK through the same upstream signaling cascade that activates NFκB pathways. JNK pathways have been implicated in a variety of biological responses. In mammals, cell differentiation, cell cycle, inflammation, and adverse environmental stimuli were shown to activate JNK signaling, although the biological outcome is often unknown (Kyriakis and Avruch, 2001; Weston and Davis, 2002). Deficiencies in JNK signaling have also been implicated in abnormal control of apoptosis. During embryonic development in *Drosophila*, JNK signaling is required for the initiation of dorsal closure, a morphological process that requires epithelial sheet movements (reviewed in Stronach and Perrimon, 1999). We have shown here that JNK pathways act downstream of microbial stimuli, both in vivo and in cells, to induce cytoskeletal regulators. In SL2 cells, JNK signaling is required for the induction of a cluster of cytoskeletal, cell adhesion regulators and proapoptotic factors. Interestingly, both NFκB and JNK branches

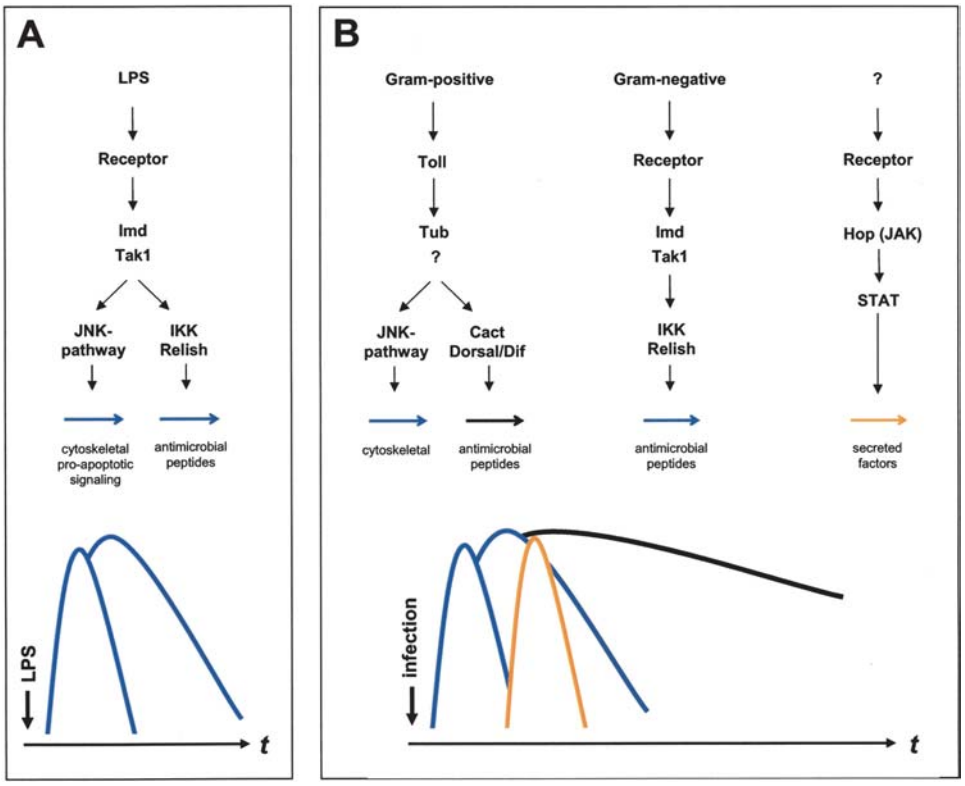

Figure 6. Model of Temporal Signaling Pathway Activation during Innate Immunity in *Drosophila*

(A) Signaling in SL2 cells in response to LPS.

(B) Signaling in adult *Drosophila* after septic injury. See text for details.

share the same upstream components, Tak1 and Imd, indicating that the activation of both processes are tightly linked. MMP-1, a matrix metalloproteinase that is one of the most markedly upregulated genes after LPS stimulation (Figure 1), has been implicated in wound-healing responses in mammals (reviewed in Raventi and Kahari, 2000). Compared with experiments in cells, the situation in vivo after septic injury is likely more complex. Gene expression profiling in whole organisms likely has a lower sensitivity for transcriptional changes that occur in rather small numbers of cells. Also, tissue-specific differences in signaling pathway activity may not reflect the transcriptional changes that we observe in our cell culture model. We found that muscle-specific cytoskeletal factors, possibly because we injected into the thoracic muscle, are not inducible in a JNK-deficient genetic background. However, since we needed to remove both Mkk4 and Hep (Mkk7) in cells to deplete JNK pathway activity, an experiment that we cannot perform in vivo because of the lack of an Mkk4 mutant, these experiments might not have uncovered all JNK-dependent transcripts. SAPK/JNK modules can also be linked to different upstream activating cascades. For example, a recent study reported the activation of p38α through a cascade involving Toll, TRAF6, and TAB (Ge et al., 2002). Similarly, during innate immune responses JNK pathways can be activated by both Toll and Imd pathways in vivo.

The activation of JNK signaling is reminiscent of signaling during dorsal and thorax closure (Stronach and Perrimon, 1999). In dorsal closure, SAPK/JNK signaling controls cytoskeletal rearrangements that lead to the epithelial sheet movements of the embryonic epidermis. In recent experiments, SAGE analysis of embryos with activated SAPK/JNK signaling show an induction of cytoskeletal factors (Jasper et al., 2001). Also, dorsal closure movements were proposed to be similar to the reepithelization that occurs during wound healing (Jacinto et al., 2001). In other developmental contexts, SAPK/JNK signaling has been implicated in cytoskeletal rearrangements and cell motility, such as the generation of planar polarity in *Drosophila* and convergent-extension movements in vertebrates (Boutros et al., 1998; Yamanaka et al., 2002). A common theme of SAPK/JNK pathways might be their control of cytoskeletal regulators for diverse biological processes. Our finding that, in response to LPS, SAPK/JNK and NFκB targets are coregulated through the same intracellular pathway suggests a close linkage of directed antimicrobial activities and tissue repair processes.

In conclusion, we employed genome-wide expression profiling to examine the contribution of different signaling pathways in complex tissues and to assign targets to candidate pathways. We have used both a cell culture model system and an in vivo analysis to show the temporal order of NFκB-dependent and -independent pathways after septic injury. An interesting question that remains is, how do the extracellular events leading to pathway activation reflect the nature of the pathogen? We noticed that clean injury experiments induced a

largely overlapping set of induced genes, but to a lower extent than septic injury (data not shown). This is consistent with experiments showing that septic injury with only gram-negative *E. coli* induced both anti-gram-negative and anti-gram-positive responses (data not shown; Irving et al., 2001). Our interpretation of these results is that wounding, in itself, might be sufficient to induce a transient (and unspecific) innate immune response. However, further studies are needed to understand the nature of the inducing agent.

Analysis of signaling pathway signatures could be a useful undertaking in order to rapidly dissect complex biological processes into smaller functional modules, such as signaling cassettes that are linked to specific transcriptional responses. The analysis of signaling pathways in various biological contexts may lead to the identification of "functional signatures," such as the proposed role of JNK pathways in cytoskeletal regulation. One of the key challenges in the future will be to integrate spatial and temporal analysis of signaling pathways to build models that reflect the complexity of signaling in vivo. We propose that the biological response after microbial infection consists of a "module" that leads to the expression of antimicrobial peptides and a second module that controls cytoskeletal gene expression, reminiscent of epithelial movement and wound-healing processes. Both processes might be coupled through a common upstream signaling pathway because infections often occur through a breach of epithelial structures.

Experimental Procedures

Drosophila Strains and Septic Injury Experiments

All flies were reared at 23°C, unless otherwise noted. Oregon R was used for wild-type experiments. The following mutant *Drosophila* strains were used in the described experiments: tub^{118}/tub^{238}, $cact^{EH9}/cact^{A2}$, key^{1}/key^{1}, rel^{E20}/rel^{E20}, Tl^{10b}, hop^{msv1}/hop^{M38}, and hep^{1} (Hedengren et al., 1999; Lemaitre et al., 1996; Lu et al., 2001). Microbial infections with *E. coli* and *M. luteus* were done as previously described (Lemaitre et al., 1995b). In brief, a concentrated mix of gram-positive and gram-negative bacteria was obtained by pooling overnight cultures of *E. coli* and *M. luteus*. Bacterial cultures were pelleted and resuspended in one-tenth of the original volume prior to infection experiments. A thin tungsten needle (Fulham) was loaded by dipping into gram-negative/gram-positive bacteria cocktail, and septic injury experiments were performed on 5- to 7-day-old adult *Drosophila* by pricking them in the thoracic segments. At indicated time points, *Drosophila* were snap-frozen in liquid nitrogen and stored at −70°C prior to further processing.

Cell Culture and dsRNA Experiments

The LPS-responsive Schneider SL2 cell line (a gift from Katja Brueckner) was cultured in Schneider's medium (GibcoBRL) supplemented with 10% fetal bovine serum (JRH Bioscience) and Penicillin-Streptomycin (GibcoBRL) at 25°C, unless noted otherwise. One day before the addition of dsRNA, 10^6 cells were seeded in 3 cm cell culture dishes (Falcon). The next day, cells were washed twice in DES medium (Sigma) without serum before treatment with 15 μg dsRNA in 1 ml DES medium. After 45 min, 2 ml of serum-supplemented Schneider's medium was added to each well, and cells were incubated for a further 72 hr to ensure protein depletion. Cells were then used in LPS (*E. coli* strain O55:B5 [Sigma], 10 μg/ml) stimulation and control experiments. dsRNA was generated and used essentially as previously described (Clemens et al., 2000). Briefly, gene-specific primers were designed to include T7 promotor sequences and were subsequently used to amplify fragments by PCR from genomic DNA. The PCR product was used in in vitro transcription (T7 MEGAscript Kit; Ambion) to generate both RNA strands in one reaction. RNA was purified with RNAeasy columns (Qiagen) and quality controlled by agarose gel electrophoresis. For expression profiling experiments, we pooled three 3 cm cell culture experiments for each labeling reaction. Total RNA was isolated by Trizol according for the manufacturer's specifications (GibcoBRL). At least two labeling reactions and hybridizations were performed for each experimental condition.

Oligonucleotide Microarray Hybridization

Reverse transcription and biotin labeling of 20 μg total RNA was done as described before (Wodicka et al., 1997). Twenty micrograms of cRNA was fragmented and hybridized for 16 hr at 45°C to *Drosophila* Genome GeneChips (Affymetrix), representing probes for over 13,600 known and predicted open reading frames. Microarrays were washed, stained, and scanned with a PMT-adjusted Agilent scanner according to standard GeneChip protocols (Affymetrix). At least two total RNA samples were independently labeled and used for separate GeneChip hybridizations.

Computational Analysis

Microarray Suite 4.0 (Affymetrix) was used for raw intensity value calculations. Intensity value files (CEL) were used as input for dChip (Li and Wong, 2001) to calculate model-based expression levels. Data sets were rejected when array probe or single probe outliers exceeded 1.5%. Following a per array quality control, intensity data was scaled by smoothing-spline normalization, and absolute expression values for each array were calculated with a model-based algorithm (Li and Wong, 2001). Low and negative expression values were truncated to 10. dChip probe-sensitivity indices were handled separately for adult *Drosophila* and cell culture specimen. Data sets from replicate arrays were merged after calculation of model-based expression levels. Genes were filtered by criteria that require a 90% confidence interval of a 1.4-fold change. In addition, we required that the difference in expression levels to be greater than 50. For the adult time-course analysis, we required that, to be selected, a gene must be at least twice the indicated threshold. Filtered genes for the 6 hr time point and mutant analysis have a minimum difference in expression levels of 100. Hierarchical clustering was performed with a Euclidean distance measure. To search for pattern similarities in pathway mutants, we calculated similarities by $c_i = 1/n\Sigma(x_i - \mu_x)(sp_i - \mu_{sp})/\sigma_x\sigma_{sp}$, where x is a vector of expression levels and sp is a vector representing the search pattern (Table 1).

Quantitative RT PCR

Quantitative PCR was performed according to the manufacturer's instructions. In brief, for each experiment, total RNA was isolated by Trizol (GibcoBRL) extraction from two 3 cm cell dishes. Ten micrograms of total RNA was treated for 30 min with DNase I prior to a 2 hr reverse transcription reaction by Superscript RT II (GibcoBRL), following the manufacturer's instructions. Quantitative PCR was performed with a LightCycler PCR machine and FastStart SYBR Green Kit (Roche). Melting curves were used as quality controls to exclude samples with genomic DNA content and to ensure single-product amplification. *rp49* levels were used as internal normalization controls. Data was analyzed with the LightCycler 3.0 software package (Roche).

Acknowledgments

We would like to thank Dominique Ferrandon, Dan Hultmark, Bruno Lemaitre, and David Schneider for fly strains. We are grateful to the Biopolymer Facility for use of their GeneChip workstation. We thank Marc Halfon, Bernard Mathey-Prevot, Henri Jasper, Dirk Bohmann, and Lutz Kockel for critical comments on the manuscript. H.A. is a Research Associate at the Institut National de la Recherche Agronomique. M.B. was supported by an Emmy-Noether fellowship from the Deutsche Forschungsgemeinschaft. N.P is an Investigator of the Howard Hughes Medical Institute.

Received: March 6, 2002
Revised: September 19, 2002

References

Aderem, A., and Ulevitch, R. (2000). Toll-like receptors in the induction of the innate immune response. Nature *406*, 782–787.

Akira, S., Takeda, K., and Kaisho, T. (2001). Toll-like receptors: critical proteins linking innate and acquired immunity. Nat. Immunol. *2*, 675–680.

Alexopoulou, L., Holt, A.C., Medzhitov, R., and Flavell, R.A. (2001). Recognition of double-stranded RNA and activation of NF-kappaB by Toll-like receptor 3. Nature *413*, 732–738.

Anderson, K.V., Bokla, L., and Nusslein-Volhard, C. (1985). Establishment of dorsal-ventral polarity in the *Drosophila* embryo: the induction of polarity by the Toll gene product. Cell *42*, 791–798.

Barillas-Mury, C., Han, Y.S., Seeley, D., and Kafatos, F.C. (1999). Anopheles gambiae Ag-STAT, a new insect member of the STAT family, is activated in response to bacterial infection. EMBO J. *18*, 959–967.

Boutros, M., Paricio, N., Strutt, D.I., and Mlodzik, M. (1998). Dishevelled activates JNK and discriminates between JNK pathways in planar polarity and wingless signaling. Cell *94*, 109–118.

Chu, S., DeRisi, J., Eisen, M., Mulholland, J., Botstein, D., Brown, P.O., and Herskowitz, I. (1998). The transcriptional program of sporulation in budding yeast. Science *282*, 699–705.

Clemens, J.C., Worby, C.A., Simonson-Leff, N., Muda, M., Maehama, T., Hemmings, B.A., and Dixon, J.E. (2000). Use of double-stranded RNA interference in *Drosophila* cell lines to dissect signal transduction pathways. Proc. Natl. Acad. Sci. USA *97*, 6499–6503.

De Gregorio, E., Spellman, P.T., Rubin, G.M., and Lemaitre, B. (2001). Genome-wide analysis of the *Drosophila* immune response by using oligonucleotide microarrays. Proc. Natl. Acad. Sci. USA *98*, 12590–12595.

Dong, C., Yang, D.D., Tournier, C., Whitmarsh, A.J., Xu, J., Davis, R.J., and Flavell, R.A. (2000). JNK is required for effector T-cell function but not for T-cell activation. Nature *405*, 91–94.

Eisen, M.B., Spellman, P.T., Brown, P.O., and Botstein, D. (1998). Cluster analysis and display of genome-wide expression patterns. Proc. Natl. Acad. Sci. USA *95*, 14863–14868.

Ekengren, S., and Hultmark, D. (2001). A family of Turandot-related genes in the humoral stress response of *Drosophila*. Biochem. Biophys. Res. Commun. *284*, 998–1003.

Fearon, D.T., and Locksley, R.M. (1996). The instructive role of innate immunity in the acquired immune response. Science *272*, 50–53.

Ge, B., Gram, H., Di Padova, F., Huang, B., New, L., Ulevitch, R.J., Luo, Y., and Han, J. (2002). MAPKK-independent activation of p38alpha mediated by TAB1-dependent autophosphorylation of p38alpha. Science *295*, 1291–1294.

Georgel, P., Naitza, S., Kappler, C., Ferrandon, D., Zachary, D., Swimmer, C., Kopczynski, C., Duyk, G., Reichhart, J.M., and Hoffmann, J.A. (2001). *Drosophila* immune deficiency (IMD) is a death domain protein that activates antibacterial defense and can promote apoptosis. Dev. Cell *1*, 503–514.

Hambleton, J., Weinstein, S.L., Lem, L., and DeFranco, A.L. (1996). Activation of c-Jun N-terminal kinase in bacterial lipopolysaccharide-stimulated macrophages. Proc. Natl. Acad. Sci. USA *93*, 2774–2778.

Han, Z.S., and Ip, Y.T. (1999). Interaction and specificity of Rel-related proteins in regulating *Drosophila* immunity gene expression. J. Biol. Chem. *274*, 21355–21361.

Hayashi, F., Smith, K.D., Ozinsky, A., Hawn, T.R., Yi, E.C., Goodlett, D.R., Eng, J.K., Akira, S., Underhill, D.M., and Aderem, A. (2001). The innate immune response to bacterial flagellin is mediated by Toll-like receptor 5. Nature *410*, 1099–1103.

Hedengren, M., Asling, B., Dushay, M.S., Ando, I., Ekengren, S., Wihlborg, M., and Hultmark, D. (1999). Relish, a central factor in the control of humoral but not cellular immunity in *Drosophila*. Mol. Cell *4*, 827–837.

Hoffmann, J.A., Kafatos, F.C., Janeway, C.A., and Ezekowitz, R.A. (1999). Phylogenetic perspectives in innate immunity. Science *284*, 1313–1318.

Hou, X.S., and Perrimon, N. (1997). The JAK-STAT pathway in *Drosophila*. Trends Genet. *13*, 105–110.

Ihle, J.N. (2001). The Stat family in cytokine signaling. Curr. Opin. Cell Biol. *13*, 211–217.

Irving, P., Troxler, L., Heuer, T.S., Belvin, M., Kopczynski, C., Reichhart, J.M., Hoffmann, J.A., and Hetru, C. (2001). A genome-wide analysis of immune responses in *Drosophila*. Proc. Natl. Acad. Sci. USA *11*, 11.

Jacinto, A., Martinez-Arias, A., and Martin, P. (2001). Mechanisms of epithelial fusion and repair. Nat. Cell Biol. *3*, E117–E123.

Janeway, C.A., Jr. (1989). Approaching the asymptote? Evolution and revolution in immunology. Cold Spring Harb. Symp. Quant. Biol. *54*, 1–13.

Jasper, H., Benes, V., Schwager, C., Sauer, S., Clauder-Munster, S., Ansorge, W., and Bohmann, D. (2001). The genomic response of the *Drosophila* embryo to JNK signaling. Dev. Cell *1*, 579–586.

Kyriakis, J.M., and Avruch, J. (2001). Mammalian mitogen-activated protein kinase signal transduction pathways activated by stress and inflammation. Physiol. Rev. *81*, 807–869.

Kimbrell, D.A., and Beutler, B. (2001). The evolution and genetics of innate immunity. Nat. Rev. Genet. *2*, 256–267.

Lagueux, M., Perrodou, E., Levashina, E.A., Capovilla, M., and Hoffmann, J.A. (2000). Constitutive expression of a complement-like protein in toll and JAK gain-of-function mutants of Drosophila. Proc. Natl. Acad. Sci. USA *97*, 11427–11432.

Lemaitre, B., Kromer-Metzger, E., Michaut, L., Nicolas, E., Meister, M., Georgel, P., Reichhart, J.M., and Hoffmann, J.A. (1995a). A recessive mutation, immune deficiency (imd), defines two distinct control pathways in the *Drosophila* host defense. Proc. Natl. Acad. Sci. USA *92*, 9465–9469.

Lemaitre, B., Meister, M., Govind, S., Georgel, P., Steward, R., Reichhart, J.M., and Hoffmann, J.A. (1995b). Functional analysis and regulation of nuclear import of dorsal during the immune response in *Drosophila*. EMBO J. *14*, 536–545.

Lemaitre, B., Nicolas, E., Michaut, L., Reichhart, J.M., and Hoffmann, J.A. (1996). The dorsoventral regulatory gene cassette spatzle/Toll/cactus controls the potent antifungal response in *Drosophila* adults. Cell *86*, 973–983.

Li, C., and Wong, W.H. (2001). Model-based analysis of oligonucleotide arrays: expression index computation and outlier detection. Proc. Natl. Acad. Sci. USA *98*, 31–36.

Lu, Y., Wu, L.P., and Anderson, K.V. (2001). The antibacterial arm of the *Drosophila* innate immune response requires an IkappaB kinase. Genes Dev. *15*, 104–110.

Martin-Blanco, E., Gampel, A., Ring, J., Virdee, K., Kirov, N., Tolkovsky, A.M., and Martinez-Arias, A. (1998). puckered encodes a phosphatase that mediates a feedback loop regulating JNK activity during dorsal closure in *Drosophila*. Genes Dev. *12*, 557–570.

Michel, T., Reichhart, J.M., Hoffmann, J.A., and Royet, J. (2001). *Drosophila* Toll is activated by Gram-positive bacteria through a circulating peptidoglycan recognition protein. Nature *414*, 756–759.

Perrimon, N., and Mahowald, A.P. (1986). l(1)hopscotch, a larval-pupal zygotic lethal with a specific maternal effect on segmentation in *Drosophila*. Dev. Biol. *118*, 28–41.

Poltorak, A., He, X., Smirnova, I., Liu, M.Y., Huffel, C.V., Du, X., Birdwell, D., Alejos, E., Silva, M., Galanos, C., et al. (1998). Defective LPS signaling in C3H/HeJ and C57BL/10ScCr mice: mutations in Tlr4 gene. Science *282*, 2085–2088.

Ramet, M., Lanot, R., Zachary, D., and Manfruelli, P. (2002). JNK signaling pathway is required for efficient wound healing in Drosophila. Dev. Biol. *241*, 145–156.

Ravanti, L., and Kahari, V.M. (2000). Matrix metalloproteinases in wound repair. Int. J. Mol. Med. *6*, 391–407.

Reedy, M.C., Bullard, B., and Vigoreaux, J.O. (2000). Flightin is essential for thick filament assembly and sarcomere stability in *Drosophila* flight muscles. J. Cell Biol. *151*, 1483–1500.

Samakovlis, C., Asling, B., Boman, H.G., Gateff, E., and Hultmark, D. (1992). In vitro induction of cecropin genes—an immune response

in a *Drosophila* blood cell line. Biochem. Biophys. Res. Commun. *188*, 1169–1175.

Schnare, M., Barton, G.M., Holt, A.C., Takeda, K., Akira, S., and Medzhitov, R. (2001). Toll-like receptors control activation of adaptive immune responses. Nat. Immunol. *2*, 947–950.

Silverman, N., Zhou, R., Stoven, S., Pandey, N., Hultmark, D., and Maniatis, T. (2000). A *Drosophila* IkappaB kinase complex required for Relish cleavage and antibacterial immunity. Genes Dev. *14*, 2461–2471.

Sluss, H.K., Han, Z., Barrett, T., Davis, R.J., and Ip, Y.T. (1996). A JNK signal transduction pathway that mediates morphogenesis and an immune response in *Drosophila*. Genes Dev. *10*, 2745–2758.

Stronach, B.E., and Perrimon, N. (1999). Stress signaling in *Drosophila*. Oncogene *18*, 6172–6182.

Takeuchi, O., Hoshino, K., Kawai, T., Sanjo, H., Takada, H., Ogawa, T., Takeda, K., and Akira, S. (1999). Differential roles of TLR2 and TLR4 in recognition of gram-negative and gram-positive bacterial cell wall components. Immunity *11*, 443–451.

Vidal, S., Khush, R.S., Leulier, F., Tzou, P., Nakamura, M., and Lemaitre, B. (2001). Mutations in the *Drosophila* dTAK1 gene reveal a conserved function for MAPKKKs in the control of rel/NF-kappaB-dependent innate immune responses. Genes Dev. *15*, 1900–1912.

Weston, C.R., and Davis, R.J. (2002). The JNK signal transduction pathway. Curr. Opin. Genet. Dev. *12*, 14–21.

Wodicka, L., Dong, H., Mittmann, M., Ho, M.H., and Lockhart, D.J. (1997). Genome-wide expression monitoring in Saccharomyces cerevisiae. Nat. Biotechnol. *15*, 1359–1367.

Yamanaka, H., Moriguchi, T., Masuyama, N., Kusakabe, M., Hanafusa, H., Takada, R., Takada, S., and Nishida, E. (2002). JNK functions in the non-canonical Wnt pathway to regulate convergent extension movements in vertebrates. EMBO Rep. *3*, 69–75.